Periodica Polytechnica Civil Engineering

Experimental Investigation of Lateral Stability of a Longitudinally Assembled Girder Made of Precast Reinforced and Prestressed Concrete Parts

Wael S. Hameedi[1*], István Völgyi[1]

[1] Department of Structural Engineering, Faculty of Civil Engineering, Budapest University of Technology and Economics, Műegyetem rkp. 3, H-1111 Budapest, Hungary
[*] Corresponding author, e-mail: wael.hameedi@edu.bme.hu

Received: 25 August 2024, Accepted: 03 January 2025, Published online: 27 January 2025

Abstract

This research focuses on the lateral stability (LS) of a longitudinally assembled girder (AG), constructed for both economic and constructional purposes. The AG features a central precast prestressed concrete (PPC) beam, 34.175 meters long, extended by two precast reinforced concrete (PRC) beams, each 2.63 meters long, connected by bolted joints. A gap between the joints was filled with high-strength grout to efficiently transfer compressive stresses. The experimental study considered two types of imperfections: initial lateral imperfections in the AG and the initial tilt angle between the connected surfaces. Three tests (AG1-A, AG1-B, AG2) were performed using nondestructive loading with concrete blocks to assess LS. The first two tests were conducted on AG1, keeping the initial imperfections consistent but varying the preload on the bolts, while the third test used specimen AG2, which had greater lateral imperfection at the mid-span cross-section. Test results showed that, due to the high preload, the tilt angle imperfection had a negligible impact on the AG's lateral stability, as separation at the connections was minimal. AG1, in tests AG1-A and AG1-B, remained laterally stable throughout the entire loading process, whereas AG2 experienced stability loss due to insufficient lateral restraints, significant geometric imperfections, and eccentric loading.

Keywords

lateral stability, initial imperfection, initial sweep, assembled girders, bolted connection

1 Introduction

In the design and building of long-span structures, precast reinforced concrete (PRC) beams are frequently employed, and their use is expanding to enhance structural performance and speed up construction [1]. This type of beams can now be longer and slenderer thanks to the advancement of high-strength materials and prestress technologies [2]. Nevertheless, the structural configuration and fabrication of elongated and more slender beams have prompted inquiries regarding the occurrence of lateral instability failure, a failure mode that was not previously considered to be significant in concrete beams [3]. In addition, slenderness increases the risk of lateral torsional failure in the presence of various factors that will recover later in this paper.

The occurrence of stability failures in construction poses a potential hazard to personnel, as these failures might happen abruptly and without warning. Moreover, the occurrence of stability failures in prestressed concrete girders during the construction phase would result in significant economic consequences. These consequences would arise from various factors, including the expenses incurred due to the failure of the girder, subsequent delays in construction activities, potential damage to construction equipment, and the potential need for temporary closures of highways on which the bridge is being built [4]. There are extensive studies regarding various structural members' lateral torsional buckling failure. Comprehensive research has been conducted on lateral-torsional buckling (LTB) in steel and composite members since the 1950s, due to the inherently narrow nature of the cross-sectional geometries employed in these materials. Limited experimental investigations and findings have been conducted about the LTB characteristics of flexural structural concrete elements [5]. Notwithstanding, several researchers studied the factors that cause this type of failure in prestressed concrete beams, for instance, the impact of prestressing force on the stability of structural concrete beams has been a subject

Cite this article as: Hameedi, W. S., Völgyi, I. "Experimental Investigation of Lateral Stability of a Longitudinally Assembled Girder Made of Precast Reinforced and Prestressed Concrete Parts", Periodica Polytechnica Civil Engineering, 2025. https://doi.org/10.3311/PPci.38183

of investigation by numerous scholars since 1950s [6–8]. It has been determined that prestressed concrete flexural members, whereby the strands or tendons are adhered to the concrete, exhibit an inability to buckle due to the presence of a constraint on out-of-plane displacement originating from the pre-stressing strands [9]. [10] postulated that the application of prestressing force would not induce buckling in the structural element, while acknowledging that externally imposed loads may still lead to buckling of the same element. In addition, the lateral deformation resulting from environmental temperature influences was investigated by [11, 12] in order to assess the lateral behavior and stability of bridge girders. This investigation included a combination of three-dimensional finite element modelling and experimental data. Additionally, number of studies proposed equations to calculate the buckling load for RC beams without considering the influence of the initial geometrical imperfections [13–15]. Several researchers utilized Southwell plot, which is a widely recognized method for experimentally finding the elastic critical buckling load of a structure with initial geometrical imperfections, without the need to submit the structure to loading in close proximity to the critical point [16]. Some studies considered the results obtained from the standard version of Southwell plot is satisfactory enough [17–21]. While others have argued that and made several modifications on these plots to get a more dependable outcome [22–24]. [3, 25, 26] developed an analytical expression to calculate the buckling load for RC beams with initial geometrical imperfections such as initial sweep and initial rotation. However, limited studies focused on the imperfections' contribution to the LTB failure for concrete girders.

This paper aims to provide the scientific community with more experimental data and arguments regarding LTB and/or rollover failures due to imperfections like geometrical imperfections and to introduce a novel imperfection termed the "initial tilt angle" between the plane surfaces of the bolted connection. This imperfection arises due to the misalignment of the connection components responsible for joining the three parts together. Such imperfections may decrease the initial stiffness of the connection after the application of loads, adversely impacting the girder's lateral stability Furthermore, the study's limitations will be addressed in the conclusion section.

2 Motivation behind the proposed bolted connection

A contract to produce slender PPCGs for the purpose of erecting a hall structure with a span of 40 meters has been granted to PREbeton Zrt., a Hungarian company that specializes in prefabricated construction. However, a unique structural challenge arose as the span length of the girder exceeded the capacity of the company's prestress bench length, which is limited to 35 meters. MUROBAU Kft., another Hungarian designer company, developed an innovative solution to overcome this challenge. The essence of this solution involves creating a novel structure by adding PRC beam to each end of the central prestressed girder as an extensions. These extensions are connected to the prestressed girder using Peikko bolted connections system.

3 Experimental program

3.1 Specimen details

The experimental program consists of three tests on two AGs; the first two tests were conducted on AG1 and labeled as (AG1-A and AG1-B), while the third test was conducted on AG2 and labeled as (AG2); Both specimens consist of three parts; the central part is the longest and has a length of 34.175 meters, and it is pre-tensioned using 28 prestressing steel strands. The other two parts are the extension beams with a length of 2.63 meters each and are normally reinforced beams. The beams are longitudinaly assembled using bolted connections; it's worth mentioning that these connections are used for the first time in this study to connect PRC beams horizontally; their original purpose is to connect beams to columns and columns to columns, this connection system consists of two parts, the first part called BECO Beam Shoe, it's casted into the end part of the extension beam together with main and secondary reinforcement, while the second part called COPRA Anchoring Couplers which are casted into the end of the central beam together with the main and secondary reinforcement. Four pairs of (BECO 20H – COPRA 20H-P) are located in the upper side of each connection zone in one row pattern, two pairs of (BECO 20H – COPRA 20H-P) are placed in the middle side of each connection zone in one row pattern, while four pairs of (BECO 39H – COPRA 39H-P) are fixed in the lower side of each connection zone in two rows pattern. The bolted connection's parts plan and dimensions are shown in Fig. 1 and Tables 1, 2, respectively [27, 28], while the details of the material properties of the tested specimens are listed in Table 3. Once the curing process is completed for all three parts, the central part is positioned on two temporary supports, while the two extension parts are joined to the central part, a 50 mm gap between assembled beams is used to ensure proper grouting, which is essential for load distribution and structural integrity. This gap allows for adequate space to place and

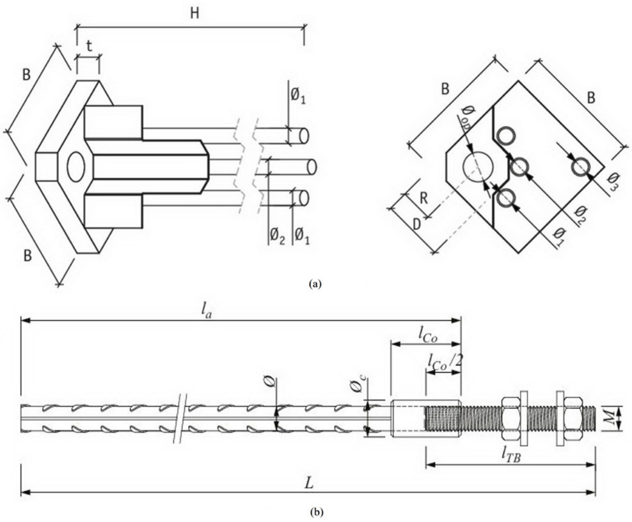

Fig. 1 Connection details

Table 1 BECO Beam Shoe dimensions (mm)

	B	H	t	R	$Ø_1$	$Ø_2$	$Ø_3$	$Ø_{op}$
BECO 20H	125	1085	20	50	16	-	12	30
BECO 39H	190	2250	45	60	32	-	28	55

Table 2 COPRA Anchoring Coupler dimensions (mm)

	M	l_{TB}	l_{Co}	$Ø_C$	Ø	l_a	L	Washer
COPRA 20H-P	M20	145	60	30	20	1200	1315	Ø44-6
COPRA 39H-P	M39	245	120	65	40	2510	2695	Ø90-10

Table 3 Material properties

Concrete quality	C50/60-XC1-16-F3
Concrete quality during tensioning	C30
Concrete cover	20 mm
Reinforcing steel	B500B
Prestressing steel strand	Y 1860 S7-12,5-R1-F1-C1
Applied prestressing force	1200 MPa

compact the grout, ensuring a strong bond and effective load transfer. It also provides tolerance for minor misalignments during assembly, making it easier to adjust the beams correctly. Additionally, the 50 mm gap helps maintain the stiffness of the connection, crucial for resisting horizontal loads and preventing excessive deformation.

After reaching the design compressive strength of the mortar the mold was detached, and the connection components on both connection zones, including bolts, washers, and nuts, underwent thorough cleaning and lubrication. Subsequently, taking into account the initial inclination imperfections of connection parts, a relatively high tightening torque of 1.2 kNm must be applied to all nuts at tests 1 and 3 to achieve firm contact and reduce the gaps that may arise due to the initial inclinations of the connection parts, while at test 2, the upper row of the bottom connection's nuts at the outer side of the AG1 loosened to almost 1 Nm. The assembled girder is a delta-shaped girder, meaning its cross-sectional depth varies along the span length. The maximum depth occurs at midspan, while the minimum depth is at the girder's ends. This variation in depth results in differing slenderness along the span. The geometric complexity makes the calculation of the critical buckling moment extremely complex, as there is no direct theoretical formula available for this case. To address this, analysis and design software (RIB Software SE) was used to calculate the critical buckling moment, considering initial imperfections in accordance with Eurocode 2 [29]. The calculated critical buckling moment is 5478 kNm, occurring at the mid-span section, where the slenderness is minimal.

3.2 Test setup

Each specimen placed on two rigid concrete members on both sides for a simply supported condition; (400 × 400 × 10) mm rubber bearing pads placed between the girder and the support to handle the vertical compressive loads evenly and to allow horizontal movement to preserve the supports from cracking and spalling; additionally, to enhance out-of-plane torsional rigidity, fork supports are strategically positioned at both ends of the girder. These supports consist of two vertical holes, each with a 63 mm diameter, placed 19 cm from the edge of each support. Two steel bars, each 25 mm in diameter, are embedded within these holes. Subsequently, the holes are filled with grout material to ensure secure fixation. A total of ten Linear Variable Differential Transformers (LVDTs) were fixed at the girder to capture the displacements; four sensors at both connection zones to capture the separation between the connected parts and installed as follows: two at the upper side of the connection zone, and two at the lower side of the connection zone. The other two sensors are fixed at the midspan cross-section of the girder to capture the vertical and lateral deflections. Table 4 and Fig. 2 show these displacement sensors' symbols and locations. The loading process was executed using concrete blocks measuring 60 × 60 × 180 cm with a 16 kN/PC weight. The experimental setup can be seen in Fig. 3.

Table 4 LVDTs symbols and locations

Symbol	Location
RUI	Right end, upper side, inner face of the girder
RUO	Right end, upper side, outer face of the girder
RBI	Right end, bottom side, inner face of the girder
RBO	Right end, bottom side, outer face of the girder
LUI	Left end, upper side, inner face of the girder
LUO	Left end, upper side, outer face of the girder
LBI	Left end, bottom side, inner face of the girder
LBO	Left end, bottom side, outer face of the girder
Vertical displacement	Lowest corner of the bottom flange at the inner face side of the girder
Lateral displacement	Highest corner of the top flange at the outer side of the girder

3.3 Initial imperfections

The tested specimens exhibit two unregulated initial imperfections: the geometrical imperfection of the central prestressed girders and the misalignment of the bolted connection parts. Regarding the geometrical defect, it's almost impossible to manufacture a perfect prestressed concrete girder. Accidental eccentricity in this type of girder can arise from various factors, including fabrication imperfections, the eccentricity of prestressing forces applied on the tendons, cracking, and permanent deformations resulting from handling and transportation processes, and the eccentricity induced by solar radiation exclusively heating one side of the girder [4]. Based on previous studies, one of the most influential geometrical imperfections affecting the lateral stability of prestressed concrete girders is the girder's initial sweep at its mid-span cross-section [3, 25]. Due to the complicity of the girder's geometry, the initial lateral imperfection (ILI), which is the horizontal distance between the center of gravity of the girder and its roll axis at the midspan section, couldn't be measured using the classic measuring methods. Instead, a point cloud technology was employed to measure this characteristic [30, 31], which is a discrete collection of data points in space. These points represent a three-dimensional shape for the assembled girder before and during the loading process. A unique set of Cartesian coordinates (X, Y, Z) is associated with each point position. Additionally, point cloud data is generated by using

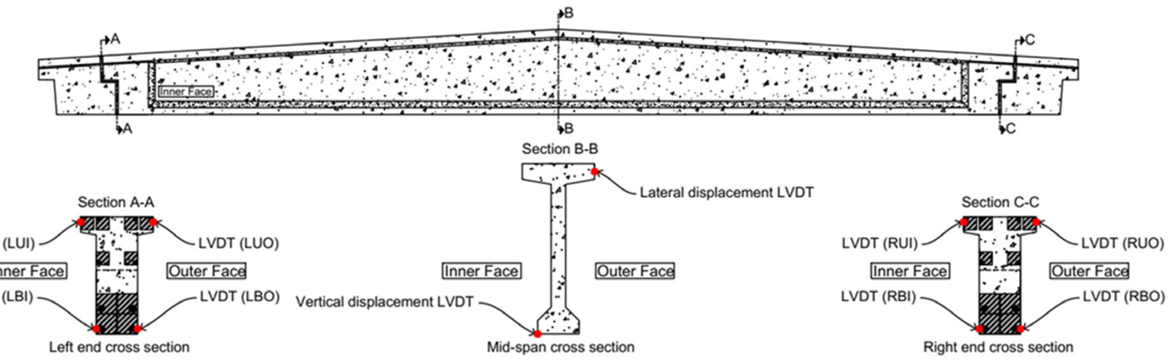

Fig. 2 Displacement sensors layout

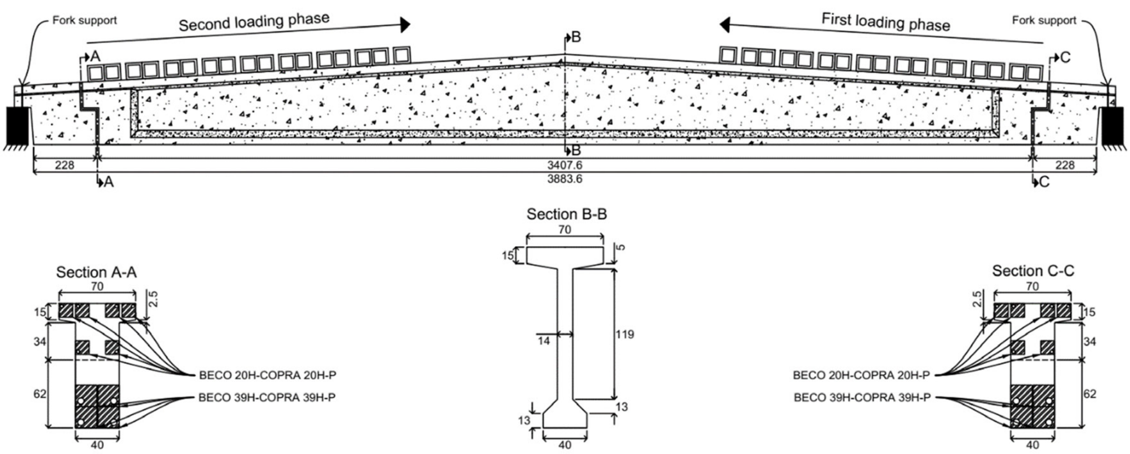

Fig. 3 Experimental setup (dimensions in cm)

a laser scanner device (Surphaser 400), as shown in Fig. 4; in Fig. 4(b), the green object represents the initial outer face of the girder before loading, while the red object represents the outer face of the girder after being fully loaded. By using AutoCAD software to compare the geometry of both objects, it becomes easier to measure the lateral deformation and twist angle during the loading process.

After processing the point cloud data, it turns out that C.G. at the midspan of AG1 initially shifted (26) mm from its roll axis, and (46) mm for AG2. It worth mentioning that fixing horizontal displacement sensors perpendicular to girder side faces can lead to errors due to the girder's lateral rotation and translation during loading, as the sensors measure diagonal instead of perpendicular distance. However, leveraging laser scan measurements provides an approach to adjust and validate sensor readings manually, minimizing error percentages associated with lateral movements during loading. The second imperfection is the initial gap or the tilt angle between the plane surfaces of the bolted connection, i.e., the error angle between the steel plate and the washer, and this is due to the inclination of beam shoe's steel plate and/or bolt, caused by the intersection between their fixing bars with the girder's main and secondary reinforcement bars. This type of imperfection is highly complicated to catch using the laser scanning technique; the author believes employing high preloads on the nuts will significantly reduce the effect of the later-mentioned imperfections of the stiffness of the connection system.

3.4 Experimental results and discussion

Generally, the loading process is divided into 18 steps. In each step, a pair of concrete blocks is placed, except for steps 9 and 18, where only a single block is placed. The first pair distanced 3.3 m from the support to avoid shear cracks at the girder's notches due to high shear forces, a tolerance distance for crane movement of 20 cm was left between loading pairs. Facing the inner face of the girder, the process begins from the right-end support and proceeds toward the mid-span, with 17 blocks placed in total. This process is then repeated in reverse, starting from the left-end support and again moving toward the mid-span, placing another 17 blocks. This results in a total of 34 blocks (535.5 kN), as illustrated in Fig. 3. After completing the loading process, the calculated bending moment at the mid-span cross-section of the girder is 3996 kNm including the self weight of the girder. As mentioned earlier, the experimental program comprises three tests: AG1-A, AG1-B, and AG2. The first two tests were conducted on specimen AG1, while the third test was conducted on specimen AG2. The details of the tests are explained as follows;

3.4.1 AG1-A Test

Prior to initiating the loading process, a relatively high preload of 1.2 kNm was applied to all connection nuts to mitigate any potential adverse effects of separations on the initial stiffness of the connections. To induce significant separations and verify the reliability of the LVDTs,

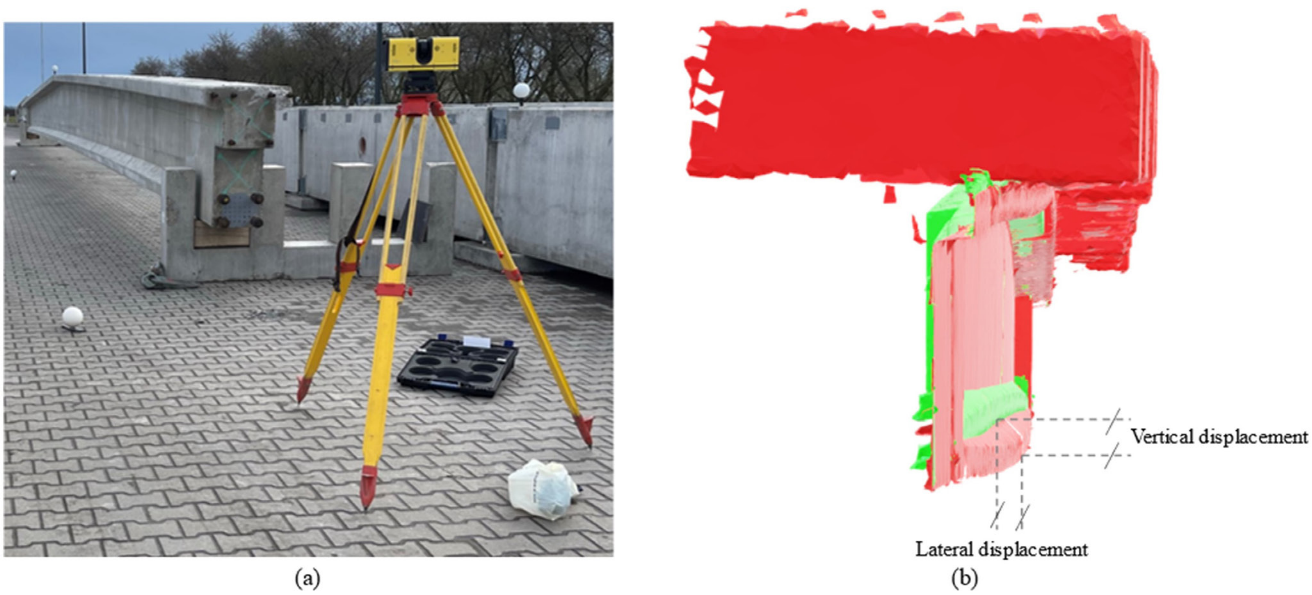

Fig. 4 3D laser scanning (a) laser scanner (b) point cloud results displaying the outer face of the girder before and after being fully loaded

the girder was loaded with 44 concrete blocks (693 kN). Following unloading in preparation for the second test, laser scan measurements revealed residual vertical and lateral deformations of 25 mm and 15 mm, respectively, which occurred as the girder entered the plastic region due to overloading. Consequently, the initial lateral imperfection of specimen AG1-B increased from 26 mm to 41 mm, measured at the center of gravity at the mid-span cross-section.

3.4.2 AG1-B Test

To investigate the impact of increased separation at both connection zones, this test aims to assess how such movement affects the initial stiffness of the connections and whether it negatively influences the lateral stability of the assembled girder, the preload of the upper row of the bottom connection's nuts at the outer side of the AG1 girder loosened to almost 1 Nm. There was a slight increase in the vertical and lateral displacements noticed at the end of this test.

3.4.3 AG2 Test

This test was performed on specimen AG2 using the same preload applied in AG1-A test. However, the initial lateral imperfection of AG2 was nearly twice that of specimen AG1. Upon fully loading the girder with 34 blocks, it experienced a loss of lateral stability as shown in Fig. 5(a), resulting in elastic buckling at a mid-span bending moment of 3996 kNm. This was lower than the critical buckling moment of 5478 kNm, as calculated using RIB SE software. The instability was attributed to several factors, including insufficient lateral restraints at the supports, caused by the complete slip of the fork support bars from the surrounding grout, as shown in Fig. 5(b). Additionally, the initial rotation of the mid-span cross-section led to the development of additional twisting moments, which were induced by the elevated center of gravity of the loading blocks. Fig. 6 presents the vertical and lateral deflections at the mid-span cross-section of the girder, along with the separations at the connection zones across all tests. In all three tests, the recorded separation values in the connection zone

(a) (b)

Fig. 5 (a) Stability failure at full loading, (b) fork support failure

did not exceed 0.6 mm, indicating that these minimal separations had a negligible impact on the lateral stability of the tested assembled girders. In Fig. 6(c), it can be seen that the lateral movement of the AG2 mid-span cross-section increased dramatically during the final steps, signaling that the girder has already lost its stability. Fig. 7 illustrates the comparison between the connection separations of AG1-A and AG1-B. As previously mentioned, these tests were performed on the same specimen, AG1. However, in the second test, AG1-B, the preload of the upper row of nuts on the bottom connection at the outer side of AG1 was loosened to approximately 1 Nm. This adjustment was intended to examine the effect of preload on the initial tensile stiffness of the bolted connection system.

The results in Fig. 7 indicate that reducing the preload of the upper row only did not impact the connection's stiffness. This is because the tensile stresses at the bottom were entirely transferred by the lower-row connections, rendering the upper-row non-essential. The upper row functions as a backup in case of potential damage, such as yielding, in the lower row connections.

4 Conclusions

This paper presents experimental results and discusses the relationship between the connections' separations and the lateral stability of the assembled girder. AG1-A and AG1-B were fully loaded with slight lateral movement due to minor initial geometrical imperfection of the mid-span cross-section. After AG2 was fully loaded with 34 blocks, it lost lateral stability and experienced elastic buckling at a mid-span bending moment of 3996 kNm. This value was lower than the critical buckling moment of 5478 kNm. The instability was caused by several issues, including inadequate lateral restraints at the supports, where the fork support bars slipped from the grout. Additionally, the initial geometrical imperfections of the mid-span cross-section introduced extra twisting moments, exacerbated by the higher C.G. of the loading blocks. The application of a high preload on the connection's nuts mitigated the adverse effects of the initial tilt angles of the connection components. This increased the initial tensile stiffness of the connections and minimized separations between the parts, rendering the impact of these separations negligible.

Further testing is required to investigate additional factors affecting the lateral stability of assembled girders with a high slenderness ratio, such as the magnitude of the preload applied to the connection nuts. The best approach for these future studies is to employ finite element modeling, as experimental tests with such characteristics are extremely costly.

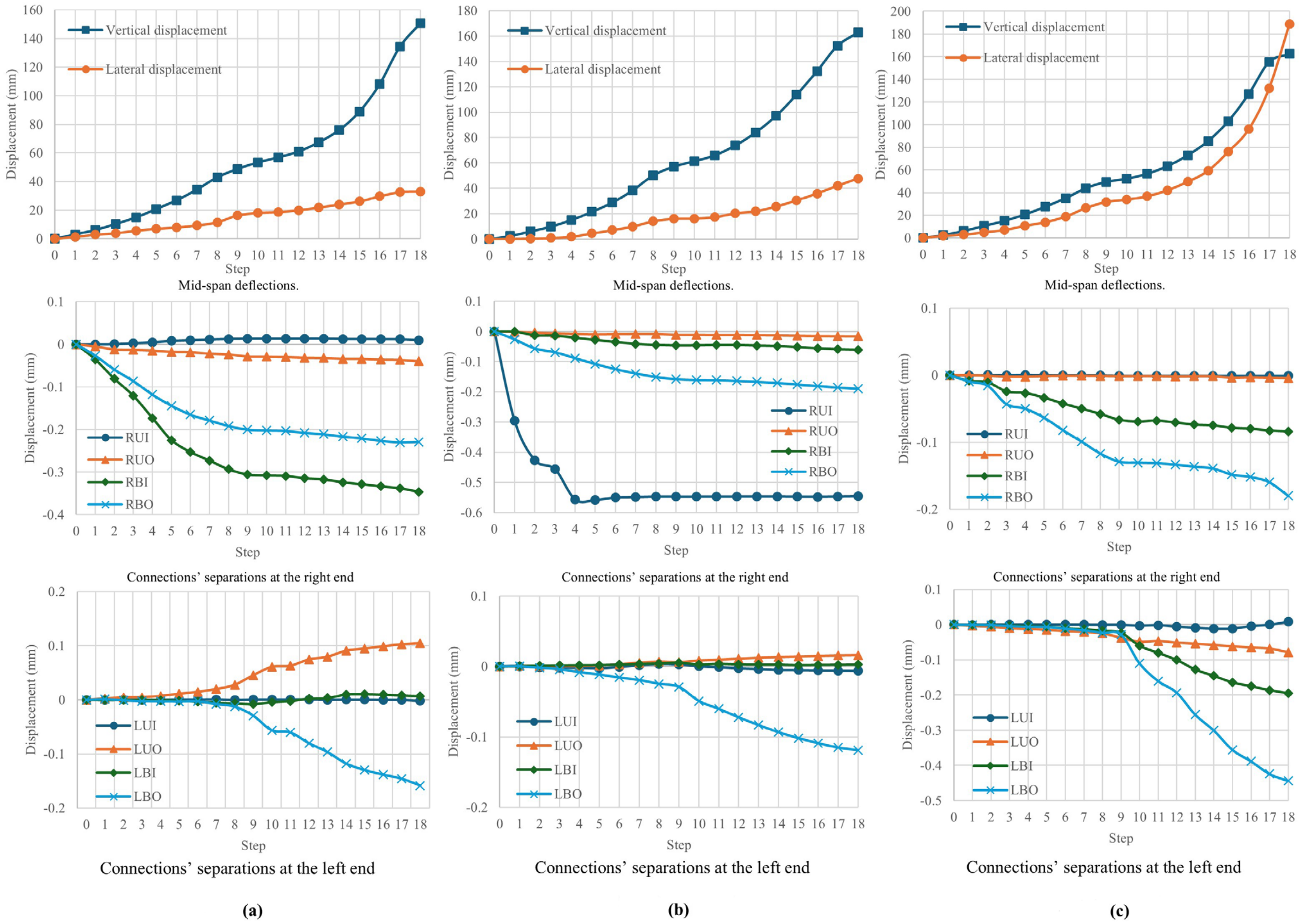

Fig. 6 Vertical, lateral deflections, and connections' separations for the tested specimens, (a) Specimen AG1-A, (b) Specimen AG1-B, (c) Specimen AG2

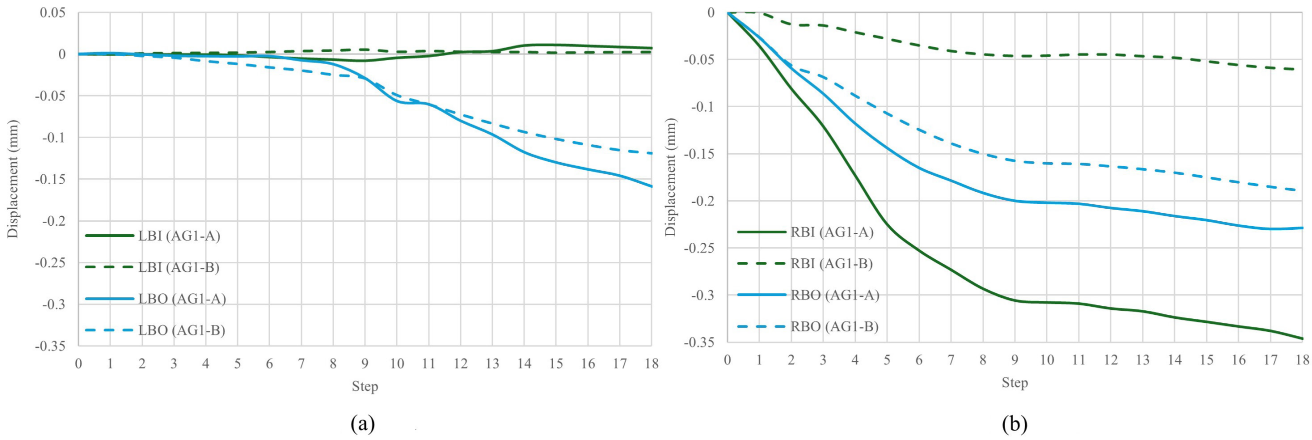

Fig. 7 Connections' separations at the bottom side of AG1-A and AG1-B for both (a) left end, (b) right end

Acknowledgments

The authors would like to express their thanks to PREbeton company staff as well as Peikko group for their contribution to accomplishing this research project. Also, the authors would like to show their appreciation to Dr. Somogyi József Árpád and Baranyai Dániel from the Department of Photogrammetry and Geoinformatics at Budapest University of Technology and Economics for their invaluable contributions in the laser scanning process.

References

[1] Lee, J. H. "Evaluation of the lateral stability of precast beams on an elastic bearing support with a consideration of the initial sweep", Engineering Structures, 143, pp. 101–112, 2017. http://doi.org/10.1016/j.engstruct.2017.04.006

[2] Krishnaraja, A. R., Kandasamy, S. "Flexural Performance of Hybrid Engineered Cementitious Composite Layered Reinforced Concrete Beams", Periodica Polytechnica Civil Engineering, 62(4), pp. 921–929, 2018. http://doi.org/10.3311/PPci.11748

[3] Lee, J. H., Kalkan, I. "Experimental and analytical investigation of lateral-torsional buckling of RC beams with geometric imperfections", Applied Mechanics and Materials, 479–480, pp. 1133–1138, 2014. http://doi.org/10.4028/www.scientific.net/AMM.479-480.1133

[4] Hurff, J. B. "Stability of Precast Prestressed Concrete Bridge Girders Considering Imperfections and Thermal Effects", PhD Thesis, Georgia Institute of Technology, 2010. [online] Available at: http://hdl.handle.net/1853/34684

[5] Hurff, J. B., Kahn, L. F. "Lateral-Torsional Buckling of Structural Concrete Beams: Experimental and Analytical Study", Journal of Structural Engineering, 138(9), pp. 1138–1148, 2012. http://doi.org/10.1061/(asce)st.1943-541x.0000542

[6] Magnel, G. "Prestressed concrete", Concrete Publications Ltd., 1950, pp. 185–191.

[7] Billig, K. "Prestressed concrete", Van Nostrand, 1953, pp. 221–222.

[8] Leonhardt, F. "Spannbeton für die praxis" (Prestressed concrete for practical use), Von Wilhelm Ernst & Sohn, 1955, pp. 373–376. (in German)

[9] Sipos, A. Á. "Calculation of the Spatial Deformations of Rods without Tensile Strength", PhD Thesis, Budapest University of Technology and Economics, 2007. [online] Available at: http://hdl.handle.net/10890/610

[10] Molke, E. C. "Auditorium Framed with Prestressed Roof Girders", ACI Journal Proceedings, 53(10), pp. 363–374, 1956. http://doi.org/10.14359/11518

[11] Lee, J. H. "Behavior of precast prestressed concrete bridge girders involving thermal effects and initial imperfections during construction", Engineering Structures, 42, pp. 1–8, 2012. https://doi.org/10.1016/j.engstruct.2012.04.003

[12] Lee, J.-H. "Investigation of Extreme Environmental Conditions and Design Thermal Gradients during Construction for Prestressed Concrete Bridge Girders", Journal of Bridge Engineering, 17(3), pp. 547–556, 2012. http://doi.org/10.1061/(ASCE)BE.1943-5592.0000277

[13] Hansell, W., Winter, G. "Lateral Stablity of Reinforced Concrete Beams", ACI Journal Proceedings, 56(9), pp. 193–214, 1959. http://doi.org/10.14359/8091

[14] Sant, J. K., Bletzacker, R. W. "Experimental Study of Lateral Stability of Reinforced Concrete Beams", ACI Journal Proceedings, 58(12), pp. 713–736, 1961. http://doi.org/10.14359/8004

[15] Massey, C. "Lateral Instablity of Reinforced Concrete Beams Under Uniform Bending Moments", ACI Journal Proceedings, 64(3), pp. 164–172, 1967. http://doi.org/10.14359/7552

[16] Mandal, P., Calladine, C. R. "Lateral-torsional buckling of beams and the Southwell plot", International Journal of Mechanical Sciences, 44(12), pp. 2557–2571, 2002. http://doi.org/10.1016/S0020-7403(02)00192-3

[17] Cheng, J. R., Yura, J. A. "Lateral Buckling Tests on Coped Steel Beams", Journal of Structural Engineering, 114(1), pp. 16–30, 1988. http://doi.org/10.1061/(ASCE)0733-9445(1988)114:1(16)

[18] Gregory, M. "The use of the Southwell Plot on strains to determine the failure load of a lattice girder when lateral buckling occurs", Australian Journal of Applied Science, 10, pp. 371–376, 1959.

[19] Gregory, M. "The application of the Southwell plot on strains to problems of elastic instability of framed structures", Australian Journal of Applied Science, 11, pp. 49–64, 1960.

[20] Dumont, C., Hill, H. N. "The lateral stability of equal-flanged aluminum-alloy I-beams subjected to pure bending", National Advisory Committee for Aeronautics, 1940.

[21] Lundquist, E. E. "Generalized analysis of experimental observations in problems of elastic stability", National Advisory Committee for Aeronautics, 1938.

[22] Massey, C. „Elastic and inelastic lateral instability of I-beams", The Engineer, 216(5622), pp. 672–674, 1963.

[23] Stratford, T. J., Burgoyne, C. J., Taylor, H. P. J., Southwell, R. V. "Stability design of long precast concrete beams", Proceedings of the Institution of Civil Engineers - Structures and Buildings, 134(2), pp. 155–168, 1999. http://doi.org/10.1680/istbu.1999.31382

[24] Stratford, T. J., Burgoyne, C. J. "Lateral stability of long precast concrete beams", Proceedings of the Institution of Civil Engineers - Structures and Buildings, 134(2), pp. 169–180, 1999. https://doi.org/10.1680/istbu.1999.31383

[25] Kalkan, I., Hurff, J. B. "Experimental Techniques for Lateral Stability Testing of Beams", Experimental Techniques, 39(5), pp. 36–47, 2015. https://doi.org/10.1111/j.1747-1567.2012.00863.x

[26] Kovács, Zs. A., Bódi, I. "Lateral torsional stability analysis of precast concrete hanging beams", Concrete Structures, 15, pp. 41–52, 2014. [online] Available at: http://fib.bme.hu/folyoirat/cs/cs2014.pdf

[27] Peikko Group "Technical Manual, Copra Anchoring Coupler", [pdf] Peikko Group, 2022. Available at: https://media.peikko.com/file/dl/i/0kpcRw/9cWEgrOfzeqNb__x73JoQQ/COPRAPeikkoGroup004TMAWeb.pdf?fv=c3a9

[28] Peikko Group "Technical Manual, BECO Beam Shoe", [pdf] Peikko Group, 2022. Available at: https://media.peikko.com/file/dl/i/hbvjjw/AV6i7mfGQSe1sgxUOFAioA/BECO_PEIKKO_GROUP_003_Technical_Manual_Web.pdf?fv=13db

[29] Code, P. "IS EN 1992-1-1:2005, Eurocode 2: design of concrete structures-part 1–1: general rules and rules for buildings", National Standards Authority of Ireland, Dublin, Ireland, pp. 659–668, 2005.

[30] Somogyi, J. Á., Lovas, T., Szabó-Leone, Á., Fehér, A. "Steels Specimens' Inspection with Structured Light Scanner", Periodica Polytechnica Civil Engineering, 66(4), pp. 1241–1247, 2022. http://doi.org/10.3311/PPci.20081

[31] Lovas, T., Ormandi, T., Somogyi, A. J., Baranyai, D., Tihanyi, V., Tettamanti, T. "OpenCRG Models From Different Data Sources to Support Vehicle Simulations", IEEE Access, 10, pp. 42690–42698, 2022. http://doi.org/10.1109/ACCESS.2022.3168287